System Identification of Beam-Like Structures Using Residual Indicators Derived from Stochastic Subspace Analysis

Riccardo Cirella(✉), Angelo Aloisio, and Rocco Alaggio

Dipartimento di Ingegneria Civile Edile-Architettura ed Ambientale, Università degli Studi dell'Aquila, Piazzale Pontieri, Monteluco di Roio, 67100 L'Aquila, Italy
riccardo.cirella@graduate.univaq.it

Abstract. In this paper, the parameters of numerical models of beam-like structures are estimated from scalar indicators derived from ambient vibration measurements. Parameters are estimated through an optimization process, in which indicators are taken as objective function. This approach is developed for an indicator, chosen from literature, derived from the reference-based covariance-driven stochastic subspace analysis. The reliability of the parametric identification is further estimated: the method proposed is numerically tested and then applied to a laboratory steel beam. Both simulated and measured vibration data are used to validate the practicability and accuracy of the approach.

Keywords: System identification · Operational modal analysis · Model-driven identification

1 Introduction

System identification consists in building mathematical models of dynamical systems and updating them on data observed from systems themselves [1]. This process is based on three main elements: the acquisition of system experimental data, the realization of the numerical representation of the investigated system, and the choice of a proper loss function, which expresses the discrepancy between measured data and the simulated response from the mathematical model.

Identification can therefore be considered as an optimization problem in which the minimization of the objective function $\mathcal{C}(x) : \mathcal{D} \subset \mathbb{R}^z \rightarrow \mathbb{R}$ leads to the identification of the system parameters $\hat{x} \in \mathbb{R}^z$, with z representing the number of parameters to be identified.

$$\hat{x} = \arg\min_{x \in \mathbb{R}^z} \mathcal{C}(x) \tag{1}$$

The choice of the objective function is conditioned by the data to be measured: when performing vibration tests on structures such as civil engineering ones, data

P. Rizzo and A. Milazzo (Eds.): EWSHM 2020, LNCE 128, pp. 559–568, 2021.
https://doi.org/10.1007/978-3-030-64908-1_52

collection is subjected to important constraints since often tests have to be performed under environmental excitation [2,3]. This is the reason why algorithms working with output-only measurements, such as the stochastic system identification (SSI), became very popular. Within the framework of the SSI, one of the steps involves the decomposition of the dynamic response into subspaces [4].

Focusing on this concept, it can be noted that the discrepancy between two different responses, one derived from data relating to the actual structural behavior and that simulated with numerical model, is measurable as a defect of orthogonality between the relative subspaces.

In the last decades, this approach has been deepened in the general context of structural health monitoring (SHM) [5–8], for the investigation of structural damage detection, through the introduction of sub-space based damage indicators [9–12]. As they are defined, damage indicators are well suited to be used as objective function in an identification procedure.

In this work, damage indicator from [13] is chosen as objective function to be minimized and its performance is numerically tested. The method is then validated through experimental tests on a real suspended steel beam.

Typical nomenclature of the SHM literature is assumed, referring to the actual structural behavior as referenc state and to the simulated responses as the reference states.

2 Subspace-Based Damage Indicators for Vibrating Structures

State-space representation of output-only measured vibration data corresponds to the following discrete time model, known as *discrete-time stochastic state-space model*

$$\begin{aligned} x_{k+1} &= Ax_k + v_k \\ y_k &= Cx_k + w_k \end{aligned} \tag{2}$$

with the states $x_k \in \mathbb{R}^n$, the outputs $y_k \in \mathbb{R}^r$, the state transition matrix $A \in \mathbb{R}^{n\times n}$ and the observation matrix $C \in \mathbb{R}^{r\times n}$, where r is the number of sensors and n is the system order. The process noise v_k is an unmeasured Gaussian white noise sequence with zero mean and constant covariance matrix $Q = \boldsymbol{E}(v_k v_k^T) \stackrel{\text{def}}{=} Q\delta(k-k')$, where $\boldsymbol{E}(\cdot)$ denotes the expectation operator and w_k is the measurement noise.

In [12,14] a residual function was proposed to detect changes in the system eigenstructure from measurements y_k without actually identifying the eigenstructure in the possibly damaged state. The considered residual is associated with a covariance-driven output-only subspace identification algorithm. Let $G = \boldsymbol{E}(x_{k+1}y_k^T)$ be the cross-covariance between the states and the outputs, $\Lambda_i = \boldsymbol{E}(y_k y_{k-i}^T) = CA^{i-1}G$ be the theoretical output covariances, and

$$H_{p+1,q} \overset{\text{def}}{=} \begin{bmatrix} \Lambda_1 & \Lambda_2 & \dots & \Lambda_q \\ \Lambda_2 & \Lambda_3 & \dots & \Lambda_{q+1} \\ \vdots & \vdots & \ddots & \vdots \\ \Lambda_{p+1} & \Lambda_{p+2} & \dots & \Lambda_{p+q} \end{bmatrix} \overset{\text{def}}{=} Hank(\Lambda_i) \tag{3}$$

the theoretic block Hankel matrix. Using measured data $(y_k)_{k=1,\dots,n}$, a consistent estimate $\hat{H}_{p+1,q}$ is obtained from the empirical output covariances

$$\hat{\Lambda}_i = \frac{1}{N} \sum_{k=1}^{n} y_k y_{k-1}^T \tag{4}$$

$$\hat{H}_{p+1,q} = Hank(\hat{\Lambda}_i) \tag{5}$$

The residual function, originally proposed by [12,14], compares the undamaged system, called also *reference state*, with the *damaged* or current one. The considered residual matrix can be written as

$$R_c = \hat{S}_0^T \hat{H}_{p+1,q} \tag{6}$$

where $\hat{S}^T$ is the left null space of the block Hankel matrix $\hat{H}_{p+1,q}$ in the reference state and $\hat{H}_{p+1,q}$ is the covariance block Hankel matrix in the current one; subscript c stays for *conventional*.

In practice, the excitation covariance Q may change between different measurement sessions of the system due to different environmental factors, while the excitation is still assumed to be stationary during one measurement. A change in the excitation covariance Q leads to a change in the cross-covariance between states and outputs G and thus in the Hankel matrix. Some researchers [13,15] proposed a new residual, which is robust to changing excitation. Let U_1 be the matrix of the left singular vectors obtained from an SVD of $\hat{H}_{p+1,q}$. As U_1 is a matrix with orthonormal columns, it can be regarded as independent of the excitation Q, which qualifies its use for a residual function that is robust to changes in the excitation covariance. Then, the residual matrix can be written as

$$R_r = \hat{S}_0^T U_1^T \tag{7}$$

where subscript r stays for *robust*. A subspace-based damage indicator may be defined as an arbitrary scalar function of the residual matrix.

$$I_d = f(R) \tag{8}$$

where I_d is a damage indicator, $f(.)$ an arbitrary scalar function and R the residual matrix. In the current paper, the damage test presented by Yan et al. [13] is implemented, built on the robust residuals (Eq. (7)):

$$I_{y,r} = norm(R_r) \tag{9}$$

where *norm* picks the maximum singular value of the matrix R_r.

3 Setup Description

In order to validate the method and illustrating the performance of the chosen indicator in guessing the actual values of the parameters involved, numerical and experimental test have been performed: in both the tests, the optimization procedure is applied for the identification of the Young modulus E and the mass density ρ of a suspended steel beam.

Both parameters have been discreetly varied within a range of feasible values: this allows to graphically represent the trend of the objective function and verify the possible presence of local minima. The structure considered in both numerical and experimental tests is a 2.5 m long steel IPE120 beam, with welded rectangular end plates of 200 mm × 100 mm × 5 mm. The beam is held up by two steel supports using springs. The structure corresponds to an actual experimental setup at the Dynamic Laboratory of the DICEAA, Università degli Studi dell'Aquila, Italy (Fig. 1).

(a) (b)

Fig. 1. (a) Experimental setup, (b) Experimental setup with added mass.

The data acquisition system is composed of seven vertical velocimeters, placed over the beam at equidistant positions and aligned along its longitudinal axis. The input signal is a white noise in the frequency band 0–1000 Hz applied by means of an electrodynamic shaker at the left end of the beam.

In order to perform the analyses required for the identification process, an in-plane finite element model of the beam described above has been considered (Fig. 2).

The beam has been divided in 8 beam finite elements [16], basing on the disposition of the velocimeters on the real structure. The input signal is simulated with a white noise vertical displacement, assigned to node 1. The output signals obtained from the model are the 7 vertical velocities of the nodes in positions corresponding to that of the 7 velocimeters placed over the experimental beam.

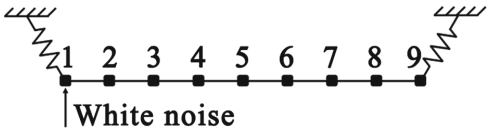

Fig. 2. Schematic representation of the FE model of the steel beam.

A constant value of 1% is taken for damping ratio for all modes involved in the analysis. Basing on laboratory experience, this value is adoptable for this kind of structure; moreover, this assumption is confirmed by results of the modal identification, described in Sect. 5.

4 Numerical Test

In order to perform the numerical test, the FE model presented in Sect. 3 has been considered. After assigning to the model a chosen value $\hat{E}$ to the Young modulus and $\hat{\rho}$ to the mass density, its dynamic response has been simulated: this response is considered as the reference state in the identification procedure.

The damaged states are produced by varying E and ρ in a discrete range of values; the objective function is then estimated comparing the damaged states to the reference.

The test was repeated several times varying the noise, in order to have a demonstration that robust indicators are indifferent to changes in noise amplitude.

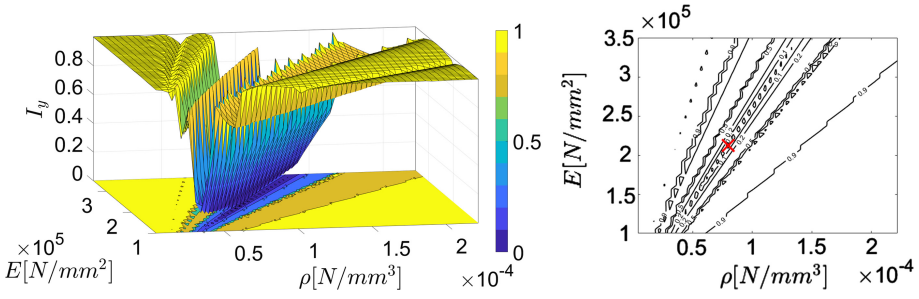

Fig. 3. Variation of the mean value of the objective function over the selected range of values for parameters E and ρ: numerical test. On the left, the trend of the objective function, on the right, the contour plot. The red cross indicates the identified point of minimum.

Figure 3 shows that the indicator presents a trend in which minima are arranged along a straight line, whose direction is that given by constant ratio between E and ρ. From the contour plot it can be seen that, in the valley, the objective function presents an absolute minimum, right in correspondence of the chosen pair $(\hat{\rho}, \hat{E})$: in the best point, the mean value of indicator is close to zero.

5 Experimental Test

The same methodology tested in the numerical case has been applied to identify the Modulus E and the mass density ρ of the experimental steel beam described in Sect. 3. In the optimization process, experimental data are used as reference state, while simulated data refers to the states produced using attempt parameters.

The identified parameters $\hat{E}$ and $\hat{\rho}$ are then compared with the pair E_{exp} and ρ_{exp}, which are respectively the conventional value of the Young modulus adopted for the steel and the measured mass density of the beam (Table 1).

Table 1. Beam parameters, frequencies and damping ratios of the first three flexural modes from modal identification, with their 2σ uncertainty bounds.

$E_{exp}\cdot 10^5$ (MPa)	$\rho_{exp}\cdot 10^{-5}$ (N/mm^3)	$f_{exp,1}$ (Hz)	$f_{exp,2}$ (Hz)	$f_{exp,3}$ (Hz)	$\xi_{exp,1}$ (%)	$\xi_{exp,2}$ (%)	$\xi_{exp,3}$ (%)
2.10	7.95	127.3 ± 0.005	337.6 ± 0.010	625.7 ± 0.007	1.28 ± 0.37	1.08 ± 0.49	0.126 ± 0.11

As a preliminary action, vibration data acquired during the experimental tests has been processed according to the SSI-COV driven algorithm, detecting the natural frequencies, the damping ratios, and the mode shapes of the steel beam. In the frequency band 0–1000 Hz, the first three modes are rigid body ones, followed by the three flexural in-plane described in Table 1 and Fig. 4.

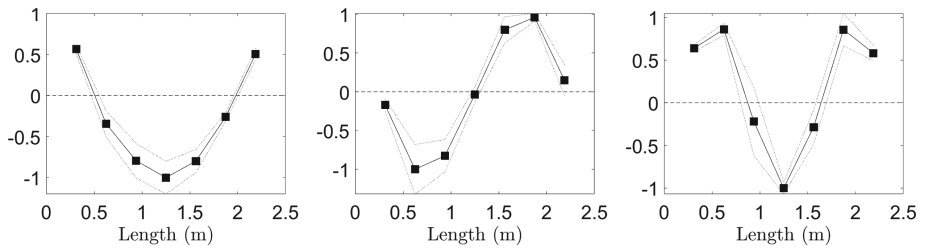

(a) 1st mode 127.3 Hz (b) 2nd mode 337.6 Hz (c) 3rd mode 625.7 Hz

Fig. 4. First three flexural in-plane mode shapes of the steel beam in the frequency range (0–1000 Hz). Full line: mode shapes, dashed line: estimated standard deviation x200.

5.1 Parametric Identification Results

Results from parametric identification (Fig. 5) show objective functions with trends similar to that obtained in numerical tests. However, unlike in the numerical case, a clear absolute minimum can't be found.

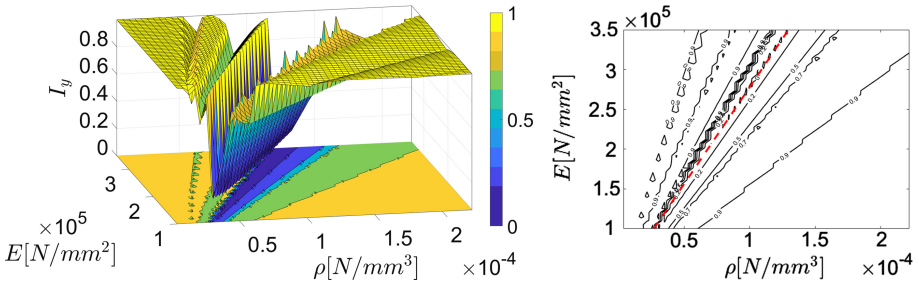

Fig. 5. Experimental test. Variation of the objective function over the selected range of values for parameters E and ρ: 3d graph (left) and relative contour plot (right).

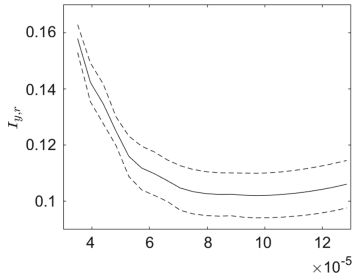

Fig. 6. Experimental test: mean value of the robust indicator along the valley and its σ bounds.

This fact can be addressed to practical problems generally relating to an experimental campaign, such as the uncertainty due to experimental measures, noise presence or other reasons, like the bias of the model or the computational uncertainty due to the chosen discretization of the parameters state $\mathcal{D}$ (Fig. 6).

Taking into account the sensitivity of the dynamics with respect to a mass variation [17], an auxiliary case is considered, in order to further constrain the solution: an additional mass of 1.4 kg/m is distributed along the beam (Fig. 3). To ensure good results, the value of the masses is chosen in a way that they produce frequency shift of about 4% [18].

The addition of the mass produces a difference in the response of the dynamic system and a consequent variation of the trend of the curves described by the objective functions: in particular, it changes the slope of the straight line that identifies the alignment of the points of minimum (Fig. 7).

Since the physical parameters to be identified do not change during the process (the total mass density is the sum of that to be identified and of a known term), the point of minimum of the objective functions has to be the same for both cases.

Therefore, it is logical to think that the pair to be identified is close to that given by the point of intersection between the two straight lines obtained (Fig. 7b).

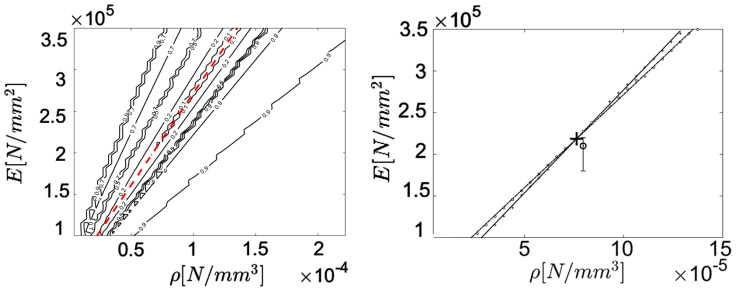

Fig. 7. (a) Results from experimental test with added mass. (b) Intersection between the lines of minima identified in the case without mass (Fig. 5) and in that with mass added (Fig. 7): the cross defines the couple of parameters identified, the circle indicates the pair (ρ_{exp}, E_{exp}). In the figure, the conventional variation interval for the Young modulus of the steel is shown.

Table 2. Experimental case: identified parameters and discrepancies with measured values.

Ind	$\hat{E}$ (MPa)	$\hat{\rho}$ (N/mm^3)	$\hat{I}_d$	E_{exp} (MPa)	ρ_{exp} (N/mm^3)	ΔE (%)	$\Delta\rho$ (%)
$I_{y,r}$	$2.19 \cdot 10^5$	$7.62 \cdot 10^{-5}$	0.109	$2.10 \cdot 10^5$	$7.925 \cdot 10^{-5}$	4.19	−3.81

Table 2 shows the pair of minimum $(\hat{E}, \hat{\rho})$ obtained from this process for both the indicators adopted and makes a comparison with the experimental one. Table 3 compares experimental modal parameters and that obtained from numerical model in which identified parameters has been applied.

Despite this discrepancy, a very small difference between the numerical and experimental frequencies and between the relative modal shapes is noted (Tables 3 and 4, Fig. 8). It's worth noticing that, while modal shapes and frequencies are almost perfectly matching, the index could be further minimized, working on the inaccuracies: this suggests that objective function based on indicators could contain more information about the system dynamics than ones based on modal properties only.

Table 3. Numerical frequencies obtained after the identification procedure and comparison with the experimental ones.

Ind	f_1 (Hz)	$f_{exp,1}$ (Hz)	Δf_1 (%)	f_2 (Hz)	$f_{exp,2}$ (Hz)	Δf_2 (%)	f_3 (Hz)	$f_{exp,3}$ (Hz)	Δf_3 (%)
$I_{y,r}$	126.6	127.3	−0.55	336.1	337.6	−0.44	625.4	625.7	$-4.8 \cdot 10^{-6}$

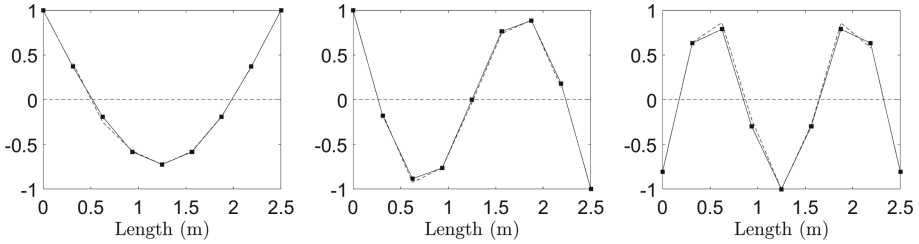

(a) 1st mode 126.6 Hz (b) 2nd mode 336.1 Hz (c) 3rd mode 625.4 Hz

Fig. 8. Mode shapes obtained from the finite element model updated using $I_{y,r}$ as objective function. The dotted line indicates the experimental shape.

Table 4. MAC matrix, calculated between numerical and experimental modes: $I_{y,r}$ indicator.

MAC	I_{num}	II_{num}	III_{num}
I_{exp}	0.9969	4.048e−04	0.2889
II_{exp}	3.014e−04	0.9980	8.896e−08
III_{exp}	0.2509	4.384e−04	0.9945

6 Conclusions

This paper presented a technique for the parametric identification of a dynamical system, assuming a residual indicator as objective function in a optimization algorithm. In the first step, the proposed method has been assessed with numerical tests on a finite-element beam model, evaluating its efficiency as objective function. Secondly, the method has been validated through an experimental test, carried out to identify the mass density and the elastic modulus of a real steel beam. Results have shown that the proposed method seems to be more sensitive to the variation of dynamic system properties than techniques which uses objective functions based only on modal parameters.

References

1. Ljung, L.: System Identification: Theory for the User. Prentice-Hall Inc., Upper Saddle River (1986)
2. Reynders, E., Pintelon, R., De Roeck, G.: Uncertainty bounds on modal parameters obtained from stochastic subspace identification. Mech. Syst. Signal Process. **22**(4), 948–969 (2008)
3. Aloisio, A., Capanna, I., Cirella, R., Alaggio, R., Di Fabio, F., Fragiacomo, M.: Identification and model update of the dynamic properties of the san silvestro belfry in l'aquila and estimation of bell's dynamic actions. Appl. Sci. **10**(12), 4289 (2020)
4. Peeters, B., De Roeck, G.: Reference-based stochastic subspace identification for output-only modal analysis. Mech. Syst. Signal Process. **13**(6), 855–878 (1999)

5. Farrar, C.R., Worden, K.: An introduction to structural health monitoring. Philos. Trans. R. Soc. A: Math. Phys. Eng. Sci. **365**(1851), 303–315 (2007)
6. Aloisio, A., Di Battista, L., Alaggio, R., Fragiacomo, M.: Sensitivity analysis of subspace-based damage indicators under changes in ambient excitation covariance, severity and location of damage. Eng. Struct. **208**, 110235 (2020)
7. Aloisio, A., Battista, L.D., Alaggio, R., Antonacci, E., Fragiacomo, M.: Assessment of structural interventions using Bayesian updating and subspace-based fault detection methods: the case study of S. Maria di Collemaggio basilica, L'aquila, Italy. Struct. Infrastruct. Eng. 1–15 (2020)
8. Antonacci, E., Aloisio, A., Galeota, D., Alaggio, R.: The S. Maria di Collemaggio basilica: from vulnerability assessment to first results of SHM. J. Architect. Eng. **26**(3), 05020007 (2020)
9. Balmès, E., Basseville, M., Bourquin, F., Mevel, L., Nasser, H., Treyssède, F.: Merging sensor data from multiple temperature scenarios for vibration monitoring of civil structures. Struct. Health Monit. **7**(2), 129–142 (2008)
10. Basseville, M., Benveniste, A., Goursat, M., Mevel, L.: Subspace-based algorithms for structural identification, damage detection, and sensor data fusion. EURASIP J. Adv. Signal Process. **2007**(1), 069136 (2006)
11. Döhler, M., Mevel, L.: Subspace-based fault detection robust to changes in the noise covariances. Automatica **49**(9), 2734–2743 (2013)
12. Basseville, M., Abdelghani, M., Benveniste, A.: Subspace-based fault detection algorithms for vibration monitoring. Automatica **36**(1), 101–109 (2000)
13. Yan, A.-M., Golinval, J.-C.: Null subspace-based damage detection of structures using vibration measurements. Mech. Syst. Signal Process. **20**(3), 611–626 (2006)
14. Basseville, M., Mevel, L., Goursat, M.: Statistical model-based damage detection and localization: subspace-based residuals and damage-to-noise sensitivity ratios. J. Sound Vibr. **275**(3–5), 769–794 (2004)
15. Döhler, M., Mevel, L., Hille, F.: Subspace-based damage detection under changes in the ambient excitation statistics. Mech. Syst. Signal Process. **45**(1), 207–224 (2014)
16. Bathe, K.-J., Wilson, E.L.: Numerical Methods in Finite Element Analysis. Prentice-Hall, Upper Saddle River (1976)
17. Parloo, E., Cauberghe, B., Benedettini, F., Alaggio, R., Guillaume, P.: Sensitivity-based operational mode shape normalisation: application to a bridge. Mech. Syst. Signal Process. **19**(1), 43–55 (2005)
18. Parloo, E.: Application of Frequency-Domain System Identification Techniques in the Field of Operational Modal Analysis. Vrije Universiteit Brussel, Brussels (2003)